ZnO(101) films by pulsed reactive crossed-beam laser ablation

S ANGAPPANE[1,2], N R SELVI[1] and G U KULKARNI[1,*]

[1]Chemistry and Physics of Materials Unit and DST Unit on Nanoscience,
Jawaharlal Nehru Centre for Advanced Scientific Research, Jakkur P.O., Bangalore 560 064, India
[2]Centre for Liquid Crystal Research, Jalahalli, Bangalore 560 013, India

Abstract. We have employed pulsed reactive crossed-beam laser ablation (PRCLA) to deposit a (101) oriented ZnO film. In this method, a supersonic jet of oxygen pulse is made to cross the laser plume from a zinc metal target while being carried to the Si(111) substrate. The obtained deposit was nanocrystalline ZnO as confirmed by a host of characterization techniques. When the substrate was held at varying temperatures, from room temperature to 900°C, the crystallinity of the obtained films increased as expected, but importantly, the crystallographic orientation of the films was varied. High substrate temperatures produced the usual (001) oriented films, while lower substrate temperatures gave rise to increasingly (101) oriented films. The substrate held at room temperature contained only the (101) orientation. The film morphology also varied with the substrate temperature, from being nanoparticulate to rod-like deposits for higher deposition temperatures. Surprisingly, the (101) orientation showed reactivity with acetone forming carbonaceous nanostructures on the surface.

Keywords. ZnO films; ZnO(101); pulsed laser deposition; reactive laser ablation; surface reactivity; carbon nanostructures.

1. Introduction

With its wide direct bandgap ($\sim 3 \cdot 37$ eV) and high exciton binding energy (~ 60 meV), zinc oxide is known to be one of the most promising oxide semiconductors with applications in light-emitting devices, window materials in solar cells, display devices, high-temperature and high-power transistors and gas sensing (Özgür *et al* 2005; Jagadish and Pearton 2006; Klingshirn 2007; Rout *et al* 2007). In recent years, various forms of ZnO, such as thin films, nanorods, nanowires, nanobelts, nanorings, nanocages, etc have been prepared by physical and chemical routes aiming at various applications (Heo *et al* 2004; Rao *et al* 2007). Diverse methods have been applied to synthesize ZnO nanostructures including solvothermal synthesis (Biswas *et al* 2008), chemical vapour deposition (Wang 2004), hydrothermal synthesis (Choy *et al* 2004), template-assisted routes (Liu *et al* 2003) and pulsed laser deposition (PLD) (Nobis *et al* 2004; Sun *et al* 2004; Angappane *et al* 2006).

Among the physical routes, pulsed laser deposition (PLD) has several advantages over the other methods. Mainly, it is versatile with the merit that it faithfully transfers the target composition to the deposited material, particularly important in doping experiments (Chrisey and Hubler 1994). Using PLD, aligned growth of ZnO nanowires and nanorods on Si substrates has been demonstrated (Nobis *et al* 2004; Sun *et al* 2004). We have synthesized ZnO pyramidal nanostructures on Si(100) substrate using PLD (Angappane *et al* 2006). The presence of droplet particulates on the film, incongruent ablation and possible oxygen deficiency in the produced films are found to be limitations of the PLD (Chen 1994). With the aim of overcoming these limitations, several modifications have been suggested for conventional PLD; off-axis PLD, magnetic-field assisted PLD, PLD with an electric field applied to the substrate, RF plasma and UV assisted PLD and pulsed reactive crossed-beam laser ablation (PRCLA) to name a few (Willmott and Huber 2000; Willmott 2004). PRCLA was first introduced by Gupta and Hussey (1991) who used pulsed high intensity jet of oxygen to make films of high-T_C superconductors by PLD. The gas pulse emerging from a nozzle valve was made to impinge at a point on the target where the laser was focused. As the plasma expands and propagates through the gas pulse, which is a transient high pressure region, it transfers some of its energy to the gas particles via collision. The gas pulse not only creates a high pressure reaction but also carries the plume and product species along towards the substrate kept parallel to the valve nozzle. PRCLA has been successfully used to reduce and deflect particulates from the deposition plume (Schenck *et al* 1998). PRCLA has also been applied to fabricate preferentially oriented films. Montenegro *et al* (2004) employed PRCLA to define the orientation of $La_{0 \cdot 6}Ca_{0 \cdot 4}CoO_3$ thin films.

*Author for correspondence (kulkarni@jncasr.ac.in)

In this article, we report our investigations on ZnO films deposited on Si(111) substrates employing PRCLA. The depositions were carried out in oxygen pulse with the substrate held at different temperatures. The obtained films have been examined employing a host of characterization techniques, XRD, SEM and TEM as well as by electrical resistivity measurements. A preliminary study has also been carried out to find out reactivity of the films. Our study has shown that depending on the substrate temperature employed during deposition, the films exhibit preferred orientations which in turn influence their reactivity pattern.

2. Experimental

Frequency tripled pulsed Nd:YAG laser (Quanta-Ray GCR-170, Spectra-Physics, USA) with a pulse width of ~5 ns and repetition rate of 10 Hz was employed for the ablation of zinc target (Johnson Matthey Co. UK, 99·99%). Pulsed supersonic valve (R.M. Jordan, USA) was placed perpendicular to the laser beam and at 45° to the plume. The Si(111) substrate was held opposite to the pulse valve at ~5 cm. Prior to mounting, the Si(111) substrate was cleaned using the piranha solution (1:2 H_2O_2:H_2O) (Caution: this mixture reacts violently with organic matter) and etched in HF (1:10 HF:H_2O) to remove residual SiO_x layer. In order to make maximum interaction of the gas pulse with plume, the distance between the pulse valve tip and the interacting point of the laser beam was optimized to less than or equal to 10 mm (Willmott and Huber 2000). Supersonic oxygen gas pulse was introduced into the chamber for 100 μs; the laser lamp was excited with 10 μs pulse with 400 μs delay and consequently Q-switch was excited with a 10 μs pulse delayed by 580 μs with respect to the pulse valve using a pulse generator (Model 9650A, EG&G, USA). These time delays were optimized for the maximum yield of the deposition onto the substrate. The pressure of the oxygen supply to the pulsed supersonic valve was kept at about 7 bar. The deposition was made at different substrate temperatures, viz. room temperature (~25°C), 400, 600, 750 and 900°C for 45 min.

The X-ray diffraction measurements were carried out on the grown films using a Miniflex (Rigaku, Japan) (CuK$_\alpha$, 1·5406 Å; scan rate, 1 deg/min) X-ray diffractometer. Scanning electron microscopy (SEM) of the films were carried out using Leica model S-440I equipment, whereas field emission scanning electron microscopy (FESEM) images were taken using the Nova NanoSEM 600 instrument (FEI Co., The Netherlands), equipped with energy dispersive X-ray (EDX) analysis (EDAX, AMETEK Inc., USA) employed for determining the surface composition of our films. Atomic force microscopy (AFM) measurements were done using a Multimode^{TM} Scanning Force Microscope attached to Nanoscope IV Controller (Digital

Instruments, USA). Transmission electron microscopy (TEM) was carried out using a JEOL 3010 operating at 300 kV on a part of the film scratched and placed on a TEM grid.

3. Results and discussion

XRD patterns of the ZnO films deposited on Si(111) substrates are shown in figure 1. The film deposited with the substrate held at room temperature (25°C) exhibits a single peak at 2θ of 36·36°, which translates to a d-spacing of 2·4679 Å. This spacing corresponds to the (101) plane of ZnO (JCPDS #36-1451). Given that the preferred growth for ZnO is along the [001] direction on various substrates
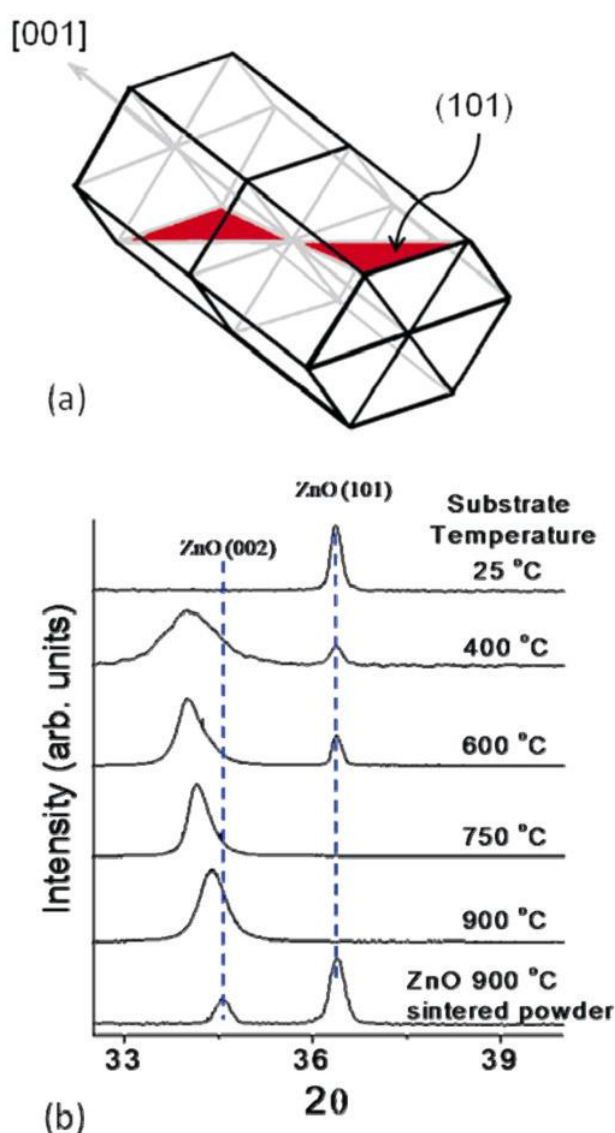

Figure 1. (**a**) ZnO unit cell showing the (101) plane and (**b**) XRD pattern of ZnO prepared by pulsed reactive crossed-beam laser ablation at various substrate temperatures. The data from a sintered powdered sample is also shown.

(Shi *et al* 2002; Kang *et al* 2004; Teng *et al* 2006), the observation is unusual. It may be noted that the (101) plane is a high density crystal plane (see the unit cell in figure 1a) showing maximum diffraction intensity in the bulk powder pattern, such as from a sintered sample also shown in figure 1b. When the substrate temperature was increased to 400°C, the XRD data shows the presence of a broad peak centred at 34·06° along with the ZnO(101) peak of diminished intensity. The former is assignable to the (002) peak of ZnO, albeit its shift (34·06° as against 34·22°). The shift and the broad nature of the peak together indicate that the ZnO species grown is in the form of nanoparticles which may be defective. For a substrate temperature of 600°C, the (002) peak becomes narrower and is shifted to higher angles, retaining the (101) peak. Interestingly, the XRD patterns obtained with the substrate deposition temperatures of 750°C and 900°C exhibit sharper (002) peaks at progressively higher angles, the (101) reflection being completely absent. Undoubtedly, these films possess increased crystallinity oriented along the *c*-axis. In another study, highly *c*-axis oriented ZnO films have been produced with the substrate being held at 400°C (Zhao *et al* 2006). It appears that under the reactive conditions adopted in our experiments, the ZnO cluster species tend to grow along the maximum density (101) plane especially when the substrate temperature is low enough not to induce annealing. An increase of the substrate temperature improves the mobility of the deposited atoms and enhances the preferred (001) directional growth of film. Previously, Fan *et al* (2005) achieved the (101) orientation by using a high laser energy density. It appears that in this case, the plasma itself carried some internal stress which induced a preferential growth. A theoretical study (Park and Park 1999) has shown that the presence of stress can alter the energetic balance between the (002) and (101) orientations.

Figure 2 shows the AFM images of the deposited films. The nanoparticulate morphology is evident in all the cases. The size of the particulate increases from 50 nm at 25°C to 90 and 100 nm with increasing substrate temperatures of 600 and 750°C, respectively. The films are generally smooth. The roughness as determined from the AFM analysis varies with the substrate temperature employed during deposition, 1·9, 3·8 and 4·2 nm for the 25, 600 and 750°C films, respectively. When the substrate temperature is increased to 900°C during PRCLA (figure 3), the deposition is less but well defined nanostructures seem to emerge as shown in the SEM image in figure 3a. Many rod-like features with sharp boundaries are seen all over the surface. The bright-field TEM image of one such rod is shown in figure 3b. Its lateral dimension is ~ 70 nm and length, ~ 100 nm. The HRTEM image in figure 3c shows the lattice fringes with a spacing of 2·6 Å from the (002) planes, indicating that the ZnO nanostructures grow along the [001] crystallographic direction. Electron diffraction pattern taken on the hexagonal structures indicate

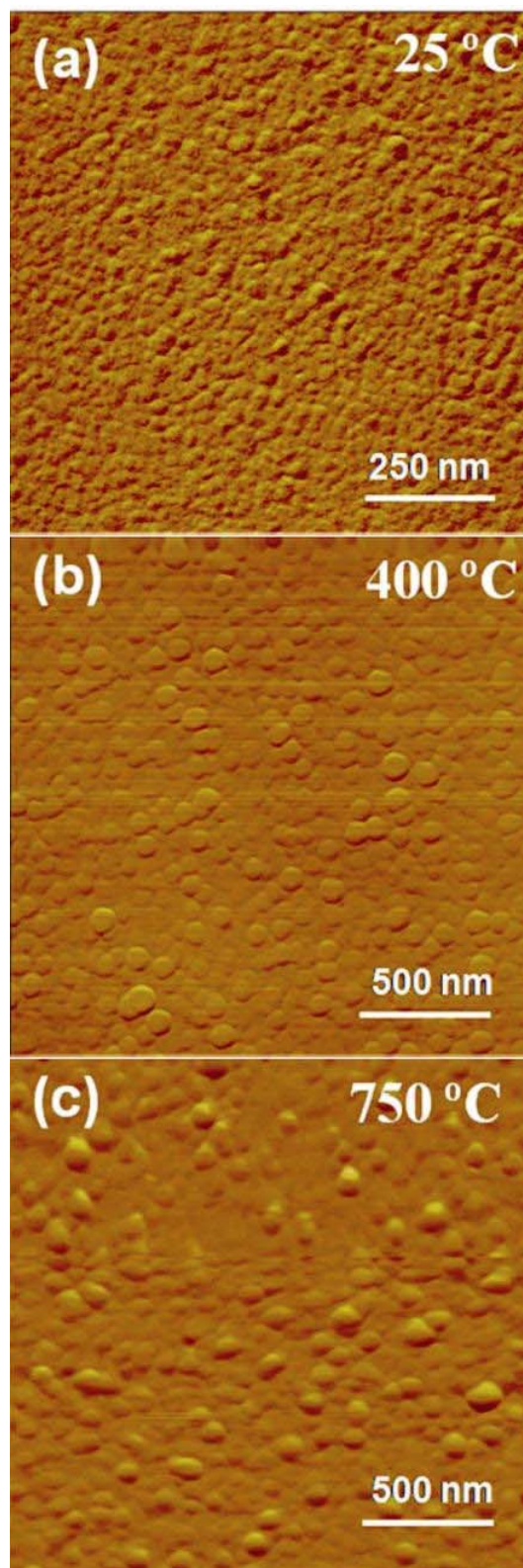[001] zone axis of ZnO crystal, consistent with the XRD result.

Figure 2. AFM images of the ZnO films deposited at (**a**) 25, (**b**) 400 and (**c**) 750°C showing surface features; the grain size is found to increase with the substrate temperature.

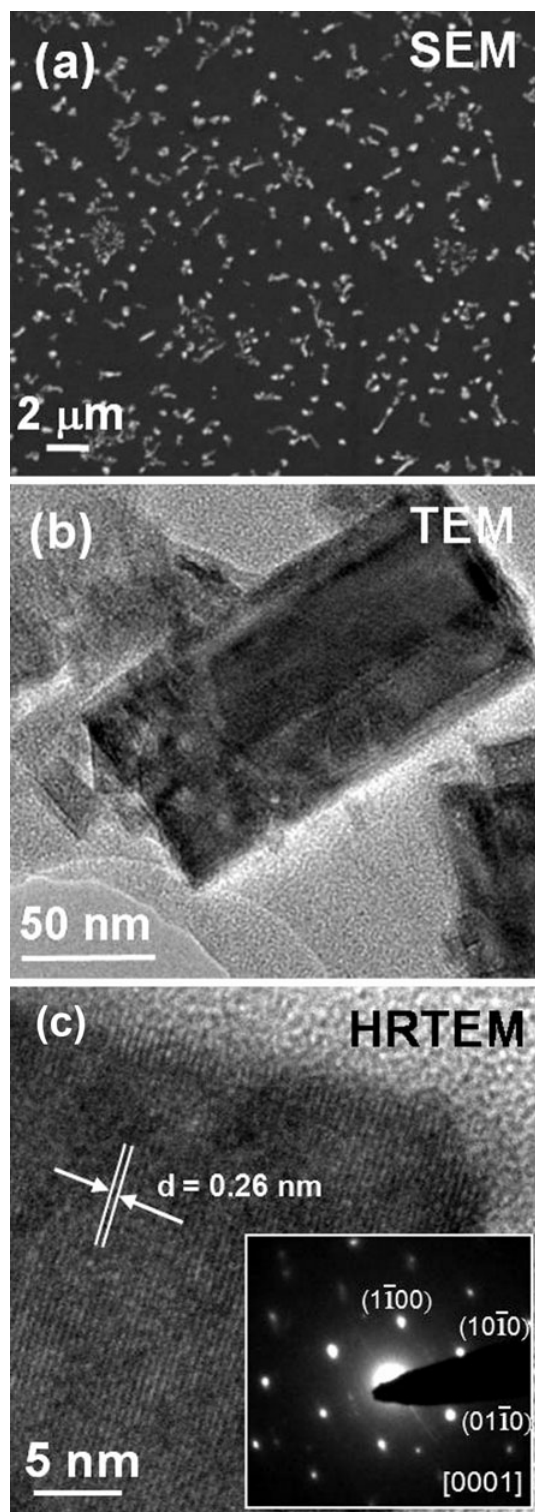The surface resistivity of the films measured by the four-probe method showed a value of 0·1 Ω-cm for the 25°C film which increased exponentially to 51·4 Ω-cm for the film deposited at 900°C (figure 4). Such an increase in the resistivity at high deposition temperatures may be due to a reduction in the number of defect electronic states (Zeng *et al* 2002). However, these values are much lower compared to the bulk ZnO resistivity of 380 Ω-cm (Maeda *et al* 2005). As the deposited films are found to contain excess oxygen (EDX value, $Zn : O = 1 : 1·7$), the resistance values are lower compared to the crystalline bulk. Higher the substrate temperature, lesser would be the density of defect electronic states which explains the increase in electrical resistivity.

We have found the ZnO(101) surfaces prepared by us to be reactive towards organic solvents such as acetone. When dipped in acetone for a few minutes, the surface was seen covered with nanostructures as shown in the SEM and AFM images in figures 5 and 6. The EDS analysis of the surface (also shown in figures 5 and 6) indicated that the new nanostructures contained predominantly carbon in some form. Such rod-like carbonaceous deposits occurred more on the surface of the 25°C film. The 400°C film also contained these nanostructures. AFM analysis showed that the structures are 50–200 nm in height and few tens of nanometers to few micrometers in length. Thus, the reactive nature of the ZnO(101) surfaces is evident. The carbon deposits are found much less on the 750°C film (figure 6), which was also subjected to acetone treatment. The structures were completely absent in the case of the 900°C film. The absence of carbonaceous deposits on the crystalline ZnO(001) surface demonstrates that the catalytic activity is unique to ZnO(101) surface which has not been reported earlier. However, the origin of such activity is unclear at present. Further studies on ZnO(101) surface are in progress using surface techniques.
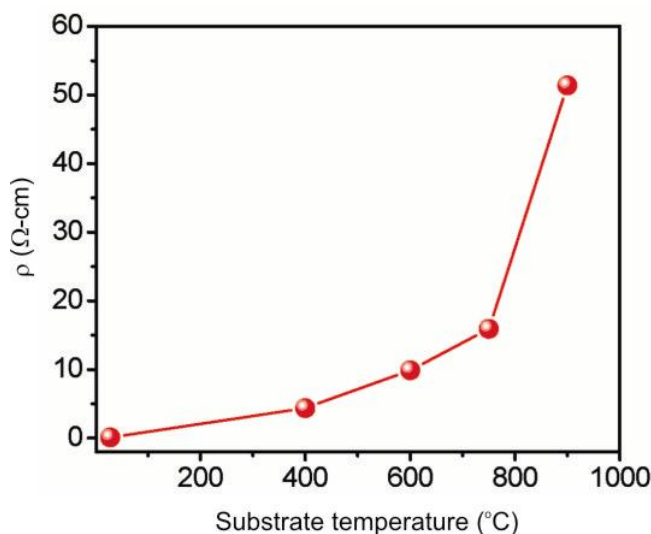

Figure 3. ZnO film deposited at 900°C: (**a**) SEM image showing nanostructures present on the surface, (**b**) TEM image of the hexagonal shaped ZnO nanorods and (**c**) HRTEM image showing lattice fringes of *c*-axis oriented ZnO. Inset shows the electron diffraction pattern of a ZnO nanorod showing *c*-axis [001] oriented growth.

Figure 4. Surface resistivity of ZnO films deposited at different substrate temperatures.
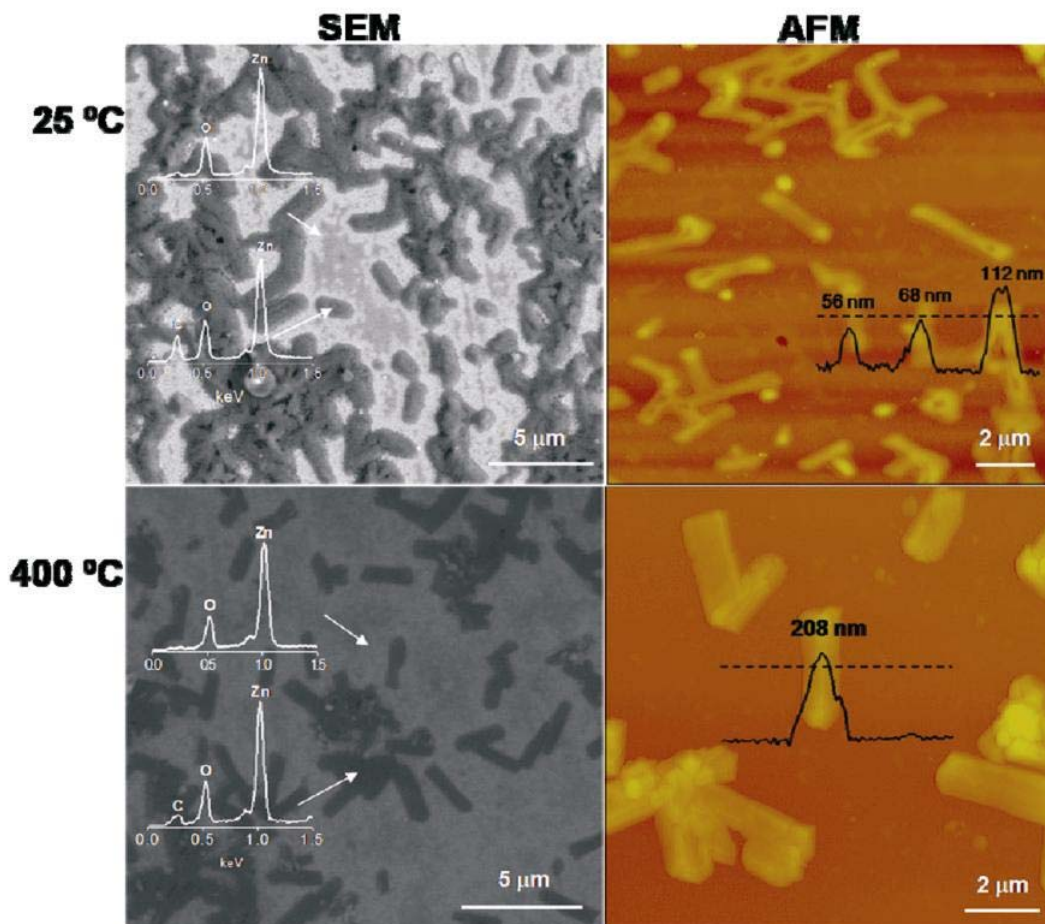
Figure 5. SEM and AFM images of the surfaces of ZnO films after being treated with acetone; bunches of carbon nanostructures are found on the surface. Insets show the EDX analysis of the surface chemical species and the AFM images are height profiles of the surface nanostructures.
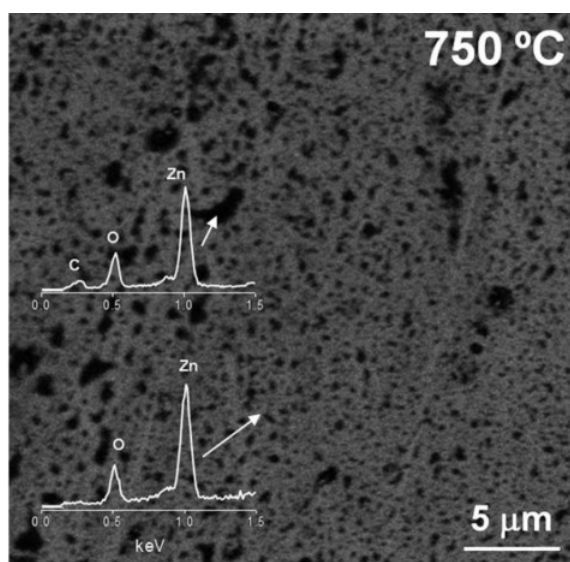

Figure 6. SEM image of the acetone treated surface of ZnO film deposited at 750°C showing very few carbon nanostructures. Insets show the EDX analysis of the surface chemical species.

4. Conclusions

We have successfully produced entirely (101) oriented ZnO films on Si(111) substrates employing pulsed reactive crossed-beam laser ablation. The favourable conditions for this process are laser plume from a Zn metal target carried to the substrate by an oxygen pulse, with the substrate being held at room temperature. The obtained film contained tightly packed nanoparticulates in the size range, 50–100 nm. With increasing substrate temperatures of 400 and 600°C, the films were of mixed orientations, (101) and (001), the latter being broad and shifted (with respect to bulk) to lower θ values due to defect nature of the particulates. At a substrate temperature of 750°C, the intensity of the (101) peak diminished with (001) becoming sharper indicating increasing crystallinity. At 900°C, the substrate produced a film entirely with the (001) orientation with larger hexagonal shaped particulates (~ 70–100 nm). Interestingly, the (101) oriented film showed high reactivity with acetone producing rod-like carbonaceous deposits, typically tens of nanometer high and few micrometer in length distributed all over

the film. The (001) orientation was found to be less reactive. Further studies are underway to explore ZnO(101) surfaces as an effective catalyst for controlled growth of carbon nanostructures.

Acknowledgements

References

Angappane S, John N S and Kulkarni G U 2006 *J. Nanosci. Nanotech.* **6** 101

Biswas K, Das B and Rao C N R 2008 *J. Phys. Chem.* **C112** 2404

Chen L C 1994 *Particulates generated by pulsed laser ablation*, in *Pulsed laser deposition of thin films* (eds) D B Chrisey and G K Hubler (New York: Wiley) p. 167

Choy J H, Jang E S, Won J H, Chung J H, Jang D J and Kim Y W 2004 *Appl. Phys. Lett.* **84** 287

Chrisey D B and Hubler G K (eds) 1994 *Pulsed laser deposition of thin films* (John Wiley & Sons)

Fan X M, Lian J S, Guo Z X and Lu H J 2005 *J. Cryst. Growth* **279** 447

Gupta A and Hussey B W 1991 *Appl. Phys. Lett.* **58** 1211

Heo Y W, Norton D P, Tien L C, Kwon Y, Kang B S, Ren F, Pearton S J and LaRoche J 2004 *Mater. Sci. Engg.* **R47** 1

Jagadish C and Pearton S J (eds) 2006 *Zinc oxide—Bulk, thin films and nanostructures* (Amsterdam: Elsevier)

Kang H S, Kang J S, Kim J W and Lee S Y 2004 *Phys. Status Solidi (c)* **1** 2550

Klingshirn C 2007 *Phys. Status Solidi (b)* **244** 3027

Liu C, Zapien J A, Yao Y, Meng X, Lee C S, Fan S, Lifshitz Y and Lee S T 2003 *Adv. Mater.* **15** 838

Maeda K, Sato M, Niikura I and Fukuda T 2005 *Semicond. Sci. Technol.* **20** S49

Montenegro M J, Lippert T, Müller S, Weidenkaff A and Wokaun A 2004 *Handai nanophotonics* (eds) H Masuhara and S Kawata **1** p. 251

Nobis T, Kaikashev E M, Rahm A, Lorenz M, Lenzner J and Grundamann M 2004 *Nanolett.* **4** 797

Özgür Ü, Alivov Ya I, Liu C, Teke A, Reshchikov M A, Doğan S, Avrutin V, Cho S-J and Morkoç H 2005 *J. Appl. Phys.* **98** 041301

Park K S and Park J K 1999 *Acta Mater.* **47** 2177

Rao C N R, Thomas P J and Kulkarni G U 2007 *Nanocrystals: synthesis, properties and applications Springer Series in Materials Science* Vol. 95

Rout C S, Kulkarni G U and Rao C N R 2007 *J. Phys. D: Appl. Phys.* **40** 2777

Schenck P K, Vaudin M D, Bonnell D W, Hastie J W and Paul A J 1998 *Appl. Surf. Sci.* **127–129** 655

Shi W S, Agyeman O and Xu C N 2002 *J. Appl. Phys.* **91** 5640

Sun Y, Fuge G M and Ashfold M N R 2004 *Chem. Phys. Lett.* **396** 21

Teng X M, Fan H T, Pan S S, Ye C and Li G H 2006 *J. Phys. D: Appl. Phys.* **39** 471

Wang Z L 2004 *Mater. Today* **7** 26

Willmott P R and Huber J R 2000 *Rev. Mod. Phys.* **72** 315

Willmott P R 2004 *Prog. Surf. Sci.* **76** 163

Zeng J N, Low J K, Ren Z M, Liew T and Lu Y F 2002 *Appl. Surf. Sci.* **197–198** 362

Zhao J, Hu L, Wang Z, Sun J and Wang Z 2006 *Appl. Surf. Sci.* **253** 841